Atmospheric
Measurement
Techniques

Development of an in situ dual-channel thermal desorption gas chromatography instrument for consistent quantification of volatile, intermediate-volatility and semivolatile organic compounds

Rebecca A. Wernis[1,2], Nathan M. Kreisberg[3], Robert J. Weber[2], Yutong Liang[2], John Jayne[4], Susanne Hering[3], and Allen H. Goldstein[1,2]

[1]Department of Civil and Environmental Engineering, University of California Berkeley, Berkeley, CA 94720, USA
[2]Department of Environmental Science, Policy and Management, University of California Berkeley, Berkeley, CA 94720, USA
[3]Aerosol Dynamics, Inc., Berkeley, CA 94710, USA
[4]Aerodyne Research, Inc., Billerica, MA 01821, USA

Correspondence: Rebecca A. Wernis (rwernis@berkeley.edu)

Abstract. Aerosols are a source of great uncertainty in radiative forcing predictions and have poorly understood health impacts. Most aerosol mass is formed in the atmosphere from reactive gas-phase organic precursors, forming secondary organic aerosol (SOA). Semivolatile organic compounds (SVOCs) (effective saturation concentration, C^*, of 10^{-1}–10^3 µg m^{-3}) comprise a large fraction of organic aerosol, while intermediate-volatility organic compounds (IVOCs) (C^* of 10^3–10^6 µg m^{-3}) and volatile organic compounds (VOCs) ($C^* \geq 10^6$ µg m^{-3}) are gas-phase precursors to SOA and ozone.

The Comprehensive Thermal Desorption Aerosol Gas Chromatograph (cTAG) is the first single instrument simultaneously quantitative for a broad range of compound-specific VOCs, IVOCs and SVOCs. cTAG is a two-channel instrument which measures concentrations of C$_5$–C$_{16}$ alkane-equivalent-volatility VOCs and IVOCs on one channel and C$_{14}$–C$_{32}$ SVOCs on the other coupled to a single high-resolution time-of-flight mass spectrometer, achieving consistent quantification across 15 orders of magnitude of vapor pressure. cTAG obtains concentrations hourly and gas–particle partitioning for SVOCs every other hour, enabling observation of the evolution of these species through oxidation and partitioning into the particle phase. Online derivatization for the SVOC channel enables detection of more polar and oxidized species.

In this work we present design details and data evaluating key parameters of instrument performance such as I/VOC collector design optimization, linearity and reproducibility of calibration curves obtained using a custom liquid evaporation system for I/VOCs and the effect of an ozone removal filter on instrument performance. Example timelines of precursors with secondary products are shown, and analysis of a subset of compounds detectable by cTAG demonstrates some of the analytical possibilities with this instrument.

1 Introduction

In recent years, understanding of organic aerosol (OA) sources has changed substantially. Globally, the burden of secondary organic constituents, i.e., those formed via atmospheric transformation processes, is much larger than that of directly emitted primary organic particulate matter. This is observed in both rural and urban areas (Docherty et al., 2008; Jimenez et al., 2009; Williams et al., 2010; Zhang et al., 2007). Volatile organic compounds (VOCs) are critical precursors to OA. VOC oxidation controls the cycling of hydroxyl and nitrogen oxide radicals and the formation of tropospheric ozone (Atkinson and Arey, 2003). The oxidation of VOCs produces lower-vapor-pressure compounds that form secondary organic aerosol (SOA) through conden-

sation onto preexisting particles, through new particle formation and growth (Seinfeld and Pankow, 2003), and through aqueous oxidation processes in aerosol or cloud water (Ervens et al., 2011). The fate of approximately half the VOC emissions entering the atmosphere cannot be observationally accounted for, and this discrepancy is likely at least partially due to a lack of comprehensive measurements of speciated organic constituents in a variety of atmospherically distinct environments (Goldstein and Galbally, 2007; Hallquist et al., 2009; Heald and Kroll, 2020).

Recent work has demonstrated that a large fraction of organic aerosol (OA) is semivolatile (Robinson et al., 2007). Intermediate-volatility organic compounds (IVOCs, defined as having an effective saturation concentration C^* of 10^3 to 10^6 µg m^{-3}) and semivolatile organic compounds (SVOCs, C^* of 10^{-1} to 10^3 µg m^{-3}) have been proposed as a substantial unaccounted for source of SOA in urban areas (Robinson et al., 2007; Weitkamp et al., 2007) but are notoriously hard to measure (Goldstein and Galbally, 2007; Hunter et al., 2017; Isaacman-VanWertz et al., 2018). This hypothesis is supported by estimates of intermediate-volatility and semivolatile organic compound (I/SVOC) abundances in the atmosphere that are an order of magnitude larger than primary organic aerosol (Robinson et al., 2007) and direct evidence that oxidation of compounds in the IVOC range efficiently produces SOA (Chan et al., 2009; de Gouw et al., 2011; Lim and Ziemann, 2009; Presto et al., 2010).

There is a need for simultaneous measurement of VOCs, IVOCs, and gas- and particle-phase SVOCs with sufficient temporal resolution to track the rapidly changing chemical composition and atmospheric conditions that directly affect SOA formation reactions. Owing to the enormous range of volatility encompassed by VOCs and I/SVOCs, this has typically been achieved through collocation of at least two separate instruments – one to measure VOCs ($C^* \geq 10^6$ µg m^{-3}) and IVOCs and another to measure SVOCs. VOCs have traditionally been measured using one of two methods. One way is to collect onto a bed of adsorbent materials and desorb and analyze into a gas chromatograph (GC) coupled to a flame ionization detector (FID) or a quadrupole mass spectrometer (MS) (e.g., Gentner et al., 2012; Goldan et al., 2004; Goldstein et al., 1995; Hopkins et al., 2003; Lamanna and Goldstein, 1999; Lerner et al., 2017; Millet et al., 2005). This method offers excellent chemical specificity as isomers are detected separately and low detection limits as samples are usually collected for many minutes before analysis. However, due to the GC temperature ramp and sample collection time, GC-based methods have a temporal resolution of 20 min to 1 h. Additionally, typically primary pollutants such as alkanes and aromatics and early-generation secondary products such as carbonyls and alcohols are measurable, but multifunctional or fully aged species are too thermally unstable or polar to measure by gas chromatography–mass spectrometry (GCMS). For example, Chung et al. (2003) were able to speciate 55 %–85 % of to-

tal VOCs at urban sites in the Los Angeles Basin, with the lower end of the range corresponding to greater photochemical processing and more of the VOC mass present in oxidized species. Another widespread method is chemical ionization mass spectrometry (CIMS), e.g., the proton transfer reaction mass spectrometer (Ionicon Analytik) and related technologies, which compared to GC-based methods offers far greater temporal resolution but less specificity as isomers cannot be separated, and detection is limited to compounds for which the ionization reaction with the chosen reagent is energetically favorable.

Particle-phase SVOCs and lower-volatility organics have traditionally been collected on disposable filters and analyzed offline via GCMS (Turpin et al., 2000). Field measurement techniques for gas- and particle-phase SVOCs have been developed relatively more recently. The FIGAERO-CIMS utilizes automated quartz filter collection for aerosol particles and controlled thermal desorption into a CIMS instrument (Lopez-Hilfiker et al., 2014), offering similar advantages and tradeoffs of CIMS applied to gas-phase measurements. The volatility and polarity separator (VAPS) sacrifices detailed speciation in order to functionally characterize a larger fraction of the organic aerosol mass (Martinez et al., 2016). The thermal desorption aerosol gas chromatograph (TAG) family of instruments, consisting of a reusable filter-based collection cell or impactor cell coupled to a GCMS, maximizes chemical speciation of gas and particle SVOCs, including separation of isomers, at hourly time resolution. The first TAG was developed by Williams et al. (2006) with the impactor cell, sensitive to particle-phase SVOCs only. Later versions incorporated an automatic liquid injection system for calibrations (Isaacman et al., 2011), a filter cell and denuder for measurement of gas-phase SVOCs and gas–particle partitioning of SVOCs (the SV-TAG; Zhao et al., 2013), a valveless injector for transferring the sample onto the GC column with minimal losses (Kreisberg et al., 2014), and online derivatization to enable detection of polar SVOCs including alkanoic acids, polyols, diacids, sugars and other multifunctional compounds in addition to nonpolar ones (Isaacman et al., 2014). A version of TAG using the impactor cell, valveless injector and online derivatization is commercially available from Aerodyne Research, Inc. Recently, an automated quartz filter collection with thermal desorption and GCMS for chemical speciation of particle-phase SVOCs has also been developed (Cropper et al., 2017; Ren et al., 2019). Using TAG with an impactor cell, Williams et al. (2010) were able to quantify an estimated 20 % of fine (PM$_1$) organic aerosol mass as measured by an aerosol mass spectrometer at an urban site. While this statistic has not been estimated directly for the SV-TAG and likely varies with the measurement location and conditions, the use of online derivatization on that instrument would increase the analyzable fraction of OA mass.

In recent years both I/VOC instruments and SVOC instruments have benefited from field-deployable high-resolution

time-of-flight mass spectrometry (HRToFMS, e.g., TOFW-ERK and IONICON Analytik). This technology affords two main advantages over quadrupole mass spectrometers. First, the high resolution ($m/\Delta m \approx 4000$ or more) allows for identification of chemical formulas of ions detected due to the unique mass defects of the different elements. Second, whereas the quadruple MS scans over a user-specified range of atomic mass units, presenting an implicit tradeoff between sensitivity and the range of possible ions detected (because a smaller range or set of discreet masses to detect allows for increased dwell times), the HRToFMS has no such limitation and allows the user to detect the entire useful range of ion masses with no compromise in sensitivity and indeed overall enhanced sensitivity.

The Comprehensive Thermal Desorption Aerosol Gas Chromatograph (cTAG) combines an I/VOC collector based upon the design of Gentner et al. (2012) and one channel of the SV-TAG joined together before a HRToFMS to access a broader volatility range of speciated organic compounds in a single instrument than previously achieved. Nonpolar and some polar VOCs and IVOCs as well as nonpolar and derivatization-amenable polar SVOCs are quantitatively collected, including many primary and secondary organics that lend insight into important sources and oxidation processes in atmospheric chemistry.

2 Description of instrument

Utilizing reusable adsorbent and stainless-steel filter collection, thermal desorption, online derivatization, GC and HRToFMS in a dual-channel setup, the cTAG measures concentrations of speciated organic compounds from C_5 through C_{32} alkane equivalent volatility. The instrument operates in an automated fashion with hourly time resolution for concentrations and gas–particle partitioning measurements of SVOCs every other hour. Derivatization of SVOCs allows for detection and analysis of polar compounds with hydroxyl groups in addition to nonpolar species. In this section, we describe the key components of the system, the sample collection, separation and detection pathways, calibration methods, timing, and data processing procedures. Figure 1 shows a schematic of the instrument.
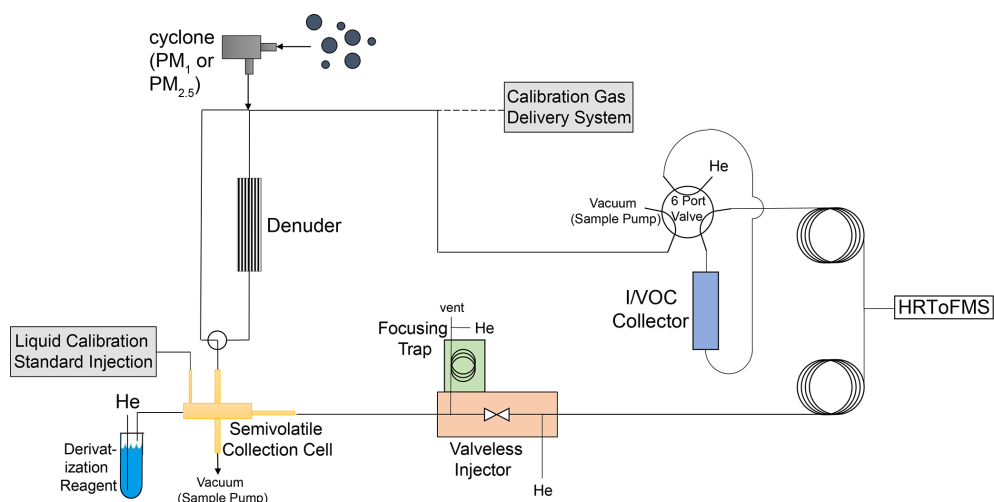
2.1 Inlet and I/VOC channel

Ambient air enters the instrument through either a sharp-cut PM$_{2.5}$ cyclone or a sharp-cut PM$_1$ cyclone depending on application-specific criteria (SCC BGI Inc., Waltham, MA) (Kenny et al., 2000). The flow is then split to collect I/VOCs and SVOCs in parallel.

On the I/VOC channel, 50 sccm of ambient air is pulled from downstream of the cyclone through a stack of three 0.25 in. diameter punches of glass fiber filters impregnated with sodium thiosulfate ($Na_2S_2O_3$) to remove ozone, fol-

lowed by a six-port valve (6PV, Valco Instruments Co. Inc.) and the I/VOC collector for I/VOC pre-concentration. The I/VOC collector consists of a layered bed of adsorbents based on the design of Gentner et al. (2012), whose types and quantities were chosen in order to efficiently collect I/VOCs with volatilities between those of n-pentane and n-hexadecane in a 1 L total sample volume when the collector is held at 30 °C. Adsorbents are layered from least to most adsorptive strength, with the IVOCs adsorbing on the least adsorptive material and the most volatile VOCs passing through and adsorbing onto the most adsorptive material. Figure 2 is a diagram of the collector. In order along the sample flow path are 60 mg glass beads (Alltech, 60/80 mesh, DCMS-treated), 10 mg Tenax TA (Supelco, 60/80 mesh), 10 mg glass beads, 20 mg Carbopack B (Supelco, 60/80 mesh), 10 mg glass beads, 20 mg Carbopack X (Supelco, 60/80 mesh) and 10 mg glass beads. The glass beads do not efficiently trap VOCs or IVOCs and serve solely as separators for the adsorbents. Once assembled and before installation on the instrument, the collector is conditioned at 325 °C with 50 sccm nitrogen for 3 h. Breakthrough volume measurements described in Sect. 3.1 were performed to ensure that this bed composition would fully collect and transfer all VOCs and IVOCs in the range of interest.

Adsorbents are packed in a custom, pure-stainless-steel housing consisting of a 3.18 mm outer diameter (o.d.) thin-walled (0.13 mm) tube brazed to a 1.59 mm o.d., 0.51 mm i.d. tube (Fig. 2). A section of the 3.18 mm portion that contains the adsorbents is flattened to 1.59 mm o.d. to reduce swept volume in the collector and improve heat transfer to enable sharper injections of highly volatile compounds. Brazing to the 1.59 mm tube eliminates the need for a union and the associated internal volume, again aiding the rapid injection of the most volatile species. A stainless-steel microfiber mesh screen (Bekaert) installed at the braze point keeps out particles and retains the adsorbents on the upstream sampling end, while a glass wool plug retains the adsorbents on the downstream end. The entire housing is chemically passivated (Inertium® treatment, AMCX, PA, USA) to prevent active compounds from reacting with the stainless steel.

During sampling the I/VOC collector is held at a temperature at least several degrees above the dew point to avoid water condensation in the system; this is typically around 30 °C. After sampling, the I/VOC collector is briefly purged with helium to reduce the amount of air and water sent to the detector. Then the 6PV actuates and helium flows through the collector in the reverse direction as the collector heats from ambient temperature to 260 °C to desorb the analytes onto the GC column (metal MXT-624, 30 m, 0.32 mm i.d., 1.8 μm phase). Two 100 W cartridge heaters mounted in an aluminum block clamped to the collector housing ensure a rapid initial heating time of 35 s, producing sharp chromatography peaks even for the unretained, most volatile species. Total desorption time is 4 min. GC analysis time is 25 min, with

Figure 1. Schematic of cTAG. VOCs and IVOCs are collected on the I/VOC collector while SVOCs are collected on the collection and thermal desorption cell. The I/VOC and SVOC channels are independent until the GC column outputs from each channel meet and enter the HRToFMS. Optionally, the SVOC channel can collect only particle-phase SVOCs by first passing sampled air through a denuder that removes all gas-phase compounds. A derivatization agent introduced upon desorption of the SVOCs from the collection cell enables detection of polar SVOCs in addition to nonpolar ones. Sample collection happens in parallel, for 23 min, followed by analysis of the I/VOC collector contents and then analysis of the semivolatile collection cell contents, for a total turnaround time of 1 h. Calibration is done for VOCs and IVOCs by manually disconnecting the ambient inlet and connecting and sampling the output of the calibration gas delivery system (Fig. 3) and for SVOCs via liquid standard injections onto the semivolatile collection cell.
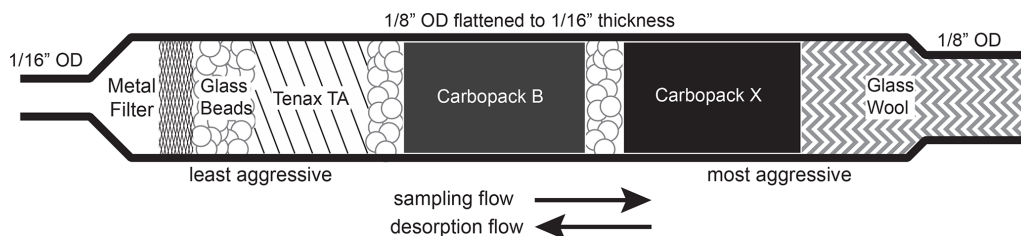
Figure 2. Schematic of I/VOC collector. Semivolatile and lower-volatility species, including particles, are captured on the metal filter. IVOCs are captured on the Tenax TA, while the most volatile analytes including isoprene are retained by the more aggressive adsorbents. Flow is reversed for desorption so that the less volatile compounds never interact with the more aggressive adsorbents.

an initial hold for 1 min at 40 °C followed by a 10 °C min^{-1} ramp to 250 °C and a 3 min hold at 250 °C.

2.2 SVOC channel

After splitting off from the combined ambient air flow through the cyclone, 10 L min^{-1} of ambient air passes through a stainless-steel filter collection and thermal desorption cell (F-CTD) maintained at 30 °C. The F-CTD quantitatively collects compounds with volatilities as high as *n*-tetradecane (C_{14}) and as low as *n*-dotriacontane (C_{32}) in the gas and particle phases.

Directly upstream of the F-CTD, an optional 500-channel activated carbon denuder (MAST Carbon) efficiently removes gas-phase species, allowing for gas–particle partitioning measurements by difference with and without the de-

nuder in line. F-CTD and denuder characteristics are described in further detail in Zhao et al. (2013).

After collection, the F-CTD is heated to 315 °C and flushed with 20–150 sccm helium during a two-stage desorption process as described in Zhao et al. (2013). Upstream of the F-CTD the helium may optionally be bubbled through a liquid reservoir of *N*-methyl-*N*-(trimethylsilyl) trifluoroacetamide (MSTFA, Sigma-Aldrich, > 98 % purity, synthesis grade) for online derivatization of species containing hydroxyl groups. Evaluation of online derivatization for TAG is discussed in Isaacman et al. (2014). The sample is reconcentrated onto a focusing trap held at 30 °C made of a 1 m metal, thick-phase chromatography column (MXT-5, 0.53 mm i.d., 5 μm phase thickness; Restek). This step allows for faster transfer of low-volatility species and efficient purging of excess derivatization agent and by-products. Flow is reversed on the trap to about 2 sccm for transfer of the sample

onto the GC column (metal MXT-5, 20 m, 0.18 mm i.d., 2 μm phase thickness; Restek) via the restrictive section of a valveless interface (VLI), described by Kreisberg et al. (2014). GC analysis time is 19 min, with an initial hold for 1 min at 50 °C followed by a 20 °C min⁻¹ ramp to 330 °C and a 4 min hold at 330 °C.

2.3 Miniature gas chromatographs

cTAG requires two separate GC columns each optimized for the separation of target species on a given channel and whose temperatures are controlled independently. In order to achieve this while preserving the instrument's compactness and time resolution, we developed miniature gas chromatographs. Each chromatograph consists of a custom machined aluminum hub around which the metal column is wrapped in a single layer so that it is in thermal contact with the hub along its entire length. On the inside surface of the hub, an expanding split-band 150 W heater heats the hub evenly around its circumference. A thermocouple inserted into a bored hole in the hub body tracks its temperature. Proportional integral derivative (PID) heating control allows for programmable, reproducible temperature ramping for GC analysis. When the temperature program completes, a fan blows ambient air onto the hub to bring it back to its initial temperature in time for the next sample injection. As with traditional GC systems, the front of the column may be trimmed (at the expense of one full winding on the aluminum hub) to extend column life. Design schematics, photos and temperature ramp reproducibility data can be found in Appendix A.

The use of miniature gas chromatographs has obvious benefits for instrument compactness and field portability. Additionally, the independent temperature control allows analysis on one channel to start while the column from the other channel is cooling down, increasing the maximum possible time resolution compared with the traditional approach of using a single oven for dual-column GC methods. While commercial miniature GC systems are available, e.g., from Valco Instruments Company Inc. (Column/Fan Modules for Fast GC, 2020), we chose to design our own for greater flexibility and the ability to use off-the-shelf columns.

2.4 High-resolution time-of-flight mass spectrometer

The two chromatography columns are joined in a passivated tee connected to an approximately 18 cm passivated stainless-steel 794 mm o.d., 125 μm i.d. tube that serves as the mass spectrometer transfer line, held at a constant 275 °C. While one column progresses through its temperature program, the other is held at its initial temperature with constant flow, and the analytes and carrier gas are pulled through the transfer line into the vacuum chamber of the mass spectrometer.

Chromatographically separated analytes are detected by a field-portable HRToFMS (TOFWERK). The HRToFMS is operated at 70 eV electron impact ionization over a user-selected mass-to-charge ratio range, typically from 15 to 450 on cTAG. This allows for matching to compounds found in mass spectral databases. For compounds not identifiable by database matching or authentic standard calibration, the mass-to-charge resolution of $m/\Delta m \approx 4000$ enables determination of the molecular formula of the ions, lending insight into molecular structure and ultimately compound identity, a critical capability for studying the complex interactions of organic molecules in the atmosphere.

2.5 Calibration

Calibration on both channels relies on injection and analysis of a suite of authentic standards in varying amounts. On the I/VOC channel, a mixture in either liquid or gas form is introduced into a custom dynamic dilution system for fine control of the output concentration. The dynamic dilution system uses a heated platinum catalyst to generate zero air at ambient relative humidity and a series of mass flow controllers (MFCs, 0–20 and 0–1000 sccm, Bronkhorst EL-FLOW) and valves to choose and dilute the input mixture for sampling (Fig. 3). Dilution ratios ranging from 50 : 1 to 1000 : 1 ensure near-ambient relative humidity for diluted mixtures. From the point of mixing to the collector, all plumbing is heated to at least 55 °C. A specialty gas cylinder with multiple components at parts-per-million levels is introduced in one port of the system.

Calibration using custom compressed gas cylinders limits the user to compounds amenable to storage in cylinders over years and does not allow significant flexibility after standard cylinders are produced. We developed a liquid evaporation system modeled after Jardine et al. (2010) to circumvent these limitations by allowing the user to purchase individual pure standards and prepare liquid solutions for evaporation and sampling. The liquid mixture is drawn into a syringe pump (TECAN Cavro Centris Pump, 250 μL glass syringe) and dispensed into another port of the dynamic dilution system at a rate of 1.6 μL min⁻¹ into a dedicated evaporation chamber. From one end of the chamber a dedicated MFC flows 1000 sccm zero air over the emerging liquid feed. Most of the resulting evaporated mixture in zero air is exhausted while 0–20 sccm is subsampled for subsequent dilution in the same manner as a gas cylinder. Once diluted, the gas or liquid calibration mixture is collected on the I/VOC collector and then desorbed and analyzed exactly like ambient air samples.

On the SVOC channel, liquid calibration mixtures are held in reservoirs pressurized under helium. A multiport selector (Rheodyne MHP7970-500-4) selects a reservoir to fill a 5 μL sample loop. A six-port valve (Rheodyne MHP9900-500-1) actuates to allow pressurized helium to push the liquid out of the loop and inject it directly onto the F-CTD via a dedicated
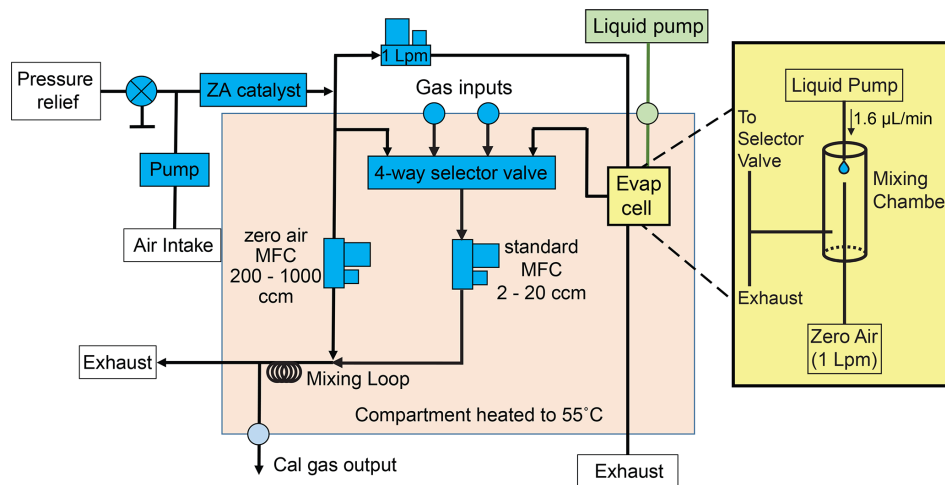
Figure 3. Schematic of dynamic dilution system for VOC and IVOC calibration. Gas cylinders or liquid mixtures can be used for calibration. Liquid mixtures are introduced into an evaporation cell using a syringe pump. The liquid is evaporated into $1\,\mathrm{L\,min^{-1}}$ of zero air to reach parts-per-million or lower concentrations. The resulting gaseous mixture (or, by user choice, the output of a calibration gas cylinder) is subsampled with a 2–$20\,\mathrm{cm^3\,min^{-1}}$ MFC and further diluted up to 500 times with more zero air before being sampled by the I/VOC collector. Zero air for the dilution system is generated by passing ambient air through a heated platinum catalyst.

port in the cell housing. A detailed description of the SVOC liquid calibration injection system may be found in Isaacman et al. (2011).

Prior to applying calibrations from analysis of authentic standards, ambient data are normalized by an internal standard introduced onto the sampling medium of each channel on every ambient sample. For the I/VOC channel, several ambient long-lived and therefore atmospherically well-mixed anthropogenic compounds with no significant current emission sources serve as suitable internal standards to control for run-to-run variability. Carbon tetrachloride is commonly used for this purpose (Lerner et al., 2017) and CFC-113 and 1,1,1-trichloroethane are also adequate for cTAG on the timescale of a typical field campaign (Engel et al., 2018; Karbiwnyk et al., 2003). The compound with the clearest signal and fewest coelutions among these is generally preferred. On the SVOC channel, a single $5\,\mu\mathrm{L}$ loop of a calibration mixture of isotopically labeled compounds spanning a variety of volatilities and functional groups is injected onto the F-CTD after collection of every ambient sample. These compounds are desorbed and analyzed with the sample and serve to track variability of derivatization efficiency and instrument response.

2.6 Instrument operation

cTAG is fully automated. All valves, fans, temperature-regulated zones and electronic pneumatic controllers are controlled by a microprocessor-based control box developed by Aerodyne Research, Inc. for commercially available TAG systems and adapted and upgraded for our system. A Microsoft Visual Basic .NET software program operating on a PC platform interfaces between the user and the control box, using serial communication to send commands and load sequences for unattended field operation and receive, display, plot, and record temperature and voltage readings.

Total turnaround time for a single instrument cycle is exactly 1 h. A typical operation sequence begins with 23 min of concurrent sampling on the I/VOC and SVOC channels with the SVOC channel optionally sampling through the denuder to remove gas-phase species. During sampling the SVOC chromatographic analysis of the previous hour's sample finishes. Once sampling is completed, the I/VOC collector is purged with helium for 1 min. Then the 6PV actuates, at which point the 25 min I/VOC GC temperature program and HRToFMS data acquisition begin and the I/VOC collector is rapidly heated to $280\,^{\circ}\mathrm{C}$ and held at that temperature for 4 min while $1.5\,\mathrm{sccm}$ of helium carries the analytes to the head of the GC column.

While the I/VOC sample is being analyzed, the SVOC liquid calibration system injects $5\,\mu\mathrm{L}$ of the internal standard mixture onto the F-CTD. The F-CTD is then heated to $315\,^{\circ}\mathrm{C}$ under 20 sccm of helium. Total helium purge flow is controlled by a mass flow controller (MFC). The flow is split downstream of the MFC, with 80 % bubbling through the reservoir of liquid derivatization agent before rejoining the other 20 % and purging the F-CTD. This flow ratio was determined to be sufficient for complete derivatization of all compound classes of interest in Isaacman et al. (2014). After 8 min, the total flow is increased to 150 sccm for 4 min to aid the transfer of the least-volatile compounds. During this process analytes are refocused on the focusing trap, held at $30\,^{\circ}\mathrm{C}$. Flow is then reversed and the trap heats to $315\,^{\circ}\mathrm{C}$ as the I/VOC GC analysis finishes. Continued purge flow from

the MFC raises the pressure in the F-CTD and forces the analytes through the restrictive portion of the VLI and onto the head of the GC column over the course of the 4 min trap desorption period. The SVOC GC analysis begins, followed by sampling for the next cycle.

A typical field campaign day sees round-the-clock sampling and analysis as previously described, alternating sampling with and without the denuder inline on the SVOC channel. Approximately every 2 weeks, calibrations are performed on both channels of the instrument simultaneously, lasting 10 to 12 h to generate multiple data points per compound for a range of loadings. The stack of sodium thiosulfate filters is replaced every 2 weeks to avoid ozone breakthrough by a safe margin (Sect. 3.4). At least once per field campaign a tank of nitrogen or zero air is plumbed into the inlet and sampled on both channels in order to quantify contaminants in the system.

2.7 Data processing

Chromatogram integrations are performed in TERN, software developed in Igor Pro 7 (WaveMetrics) by Isaacman-VanWertz et al. (2017). TERN enables automatic batch integration of single compounds on hundreds of chromatograms at a time for rapid generation of compound concentration timelines. Compounds are organized in templates, and the ability to search commercial or custom mass spectral libraries for compound identification is built in.

3 System evaluation

The focus of development and system evaluation was on the I/VOC channel, as the SVOC channel is identical to a single channel of the previously developed SV-TAG instrument extensively documented elsewhere (Isaacman et al., 2011, 2014; Kreisberg et al., 2014; Zhao et al., 2013). Development for the cTAG focused on optimizing the design of the I/VOC collector, developing a calibration system for the I/VOC channel capable of using custom liquid mixtures, ensuring removal of ozone for accurate collection of ozone-reactive VOCs and IVOCs and field deployment in a polluted urban area.

3.1 I/VOC collector breakthrough tests

The target collection range for the I/VOC channel was chosen to include isoprene, a key biogenic C_5 hydrocarbon, on the high-volatility end. The low-volatility end was chosen to overlap with the SVOC channel range (which starts at C_{14}) by several carbon numbers and to include sesquiterpenes, a class of C_{15} compounds also of biogenic origin but with greatly varying structures and reactivity and which are far less well-documented and understood (Bouvier-Brown et al., 2009; Chan et al., 2016; Yee et al., 2018).

In order to decide the final quantities of adsorbents in the I/VOC collector, three different collector compositions were tested for breakthrough of the most volatile species. Briefly, breakthrough volume is defined as the volume of carrier gas required to purge an analyte through the adsorbent bed, dependent on adsorbent quantity, temperature and analyte volatility (Definition of Breakthrough Volumes, 2020). The breakthrough volume must be larger than the volume of air sampled for the most volatile analyte of interest to ensure complete collection of all analytes.

Breakthrough volumes were measured using a real-time VOC instrument, a proton transfer reaction mass spectrometer (PTR-MS, IONICON Analytik). The output of a specialty gas cylinder of biogenic VOCs was diluted using the custom dynamic dilution system to deliver parts-per-billion-level concentrations of analytes to the collector, held via PID temperature control at 30 °C. The PTR-MS inlet was connected downstream of the prototype collector while sampling from the controlled gas mixture at 100 sccm. For each analyte, the PTR-MS measured zero concentration until the breakthrough volume was reached, after which the downstream-measured concentration rapidly rose and plateaued. The beginning of the rapid rise in concentration was taken to be the point of breakthrough.

Breakthrough volume measurement results for isoprene and the sum of methyl vinyl ketone and methacrolein (MVK+MACR) for several collector prototypes are shown in Table 1. For compactness and to reduce thermal mass to ensure rapid desorption, we targeted a final design containing the minimum quantity of adsorbents that would safely and robustly meet our requirements for breakthrough volume. Collector 3, which had the lowest quantities of adsorbents of the three different prototype collectors tested, had a breakthrough volume of twice our usual 1 L sample volume for MVK+MACR. We therefore settled on a fourth prototype with quantities intermediate between collectors 2 and 3 of the most aggressive adsorbents to ensure a safe margin. We also reduced the quantity of Tenax TA, as the 10 mg final quantity provides more-than-sufficient breakthrough volumes for the lower-volatility compounds that it collects (Tenax® TA Breakthrough Volume Data, 2020).

3.2 Dynamic dilution system testing

The dynamic dilution system for evaporation of liquid I/VOC mixtures and dilution and delivery of liquid and gas calibration mixtures was evaluated for linearity and reproducibility of delivered concentrations. In addition, for compounds present in both gas cylinders and liquid solutions calibration curves were compared for agreement. Calibrant compounds from liquid (prepared in lab) and gas cylinder (Custom mixture prepared by Apel-Riemer Environmental, Inc., 2019) mixtures were introduced at 0, 1, 2, 4, 8 and 12 ppb (10 times lower concentration for β-caryophyllene) with a total volume of air sampled of 280 cm^3 with six (0, 1, 2, 4,

Table 1. Composition of different I/VOC collectors and corresponding breakthrough volumes for some of the most volatile target compounds. Collector 4 is a compromise between collectors 2 and 3 with reduced Tenax TA.
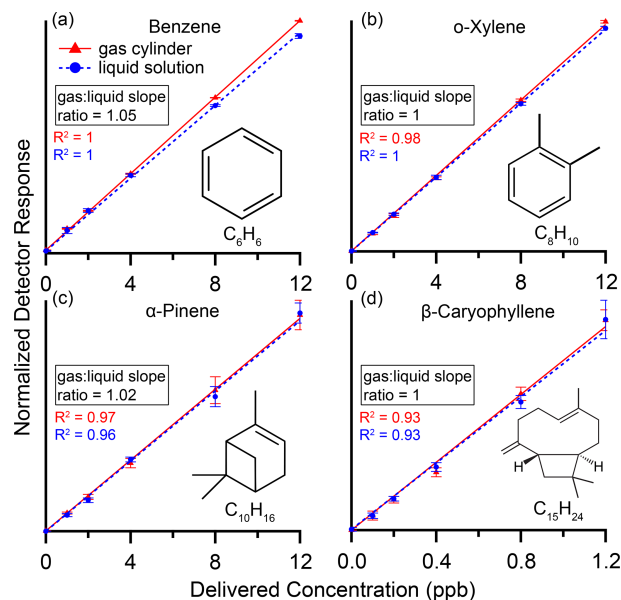
Collector no.	1	2	3	4
Bed material (mg of sorbent)				
Glass beads	40	40	40	40
Tenax TA	20	20	20	10
Carbopack B	30	20	10	20
Carbopack X	40	30	15	20
Breakthrough volume at 30 °C (L)				
MVK+MACR	13.2	8.7	2.0	>2
Isoprene	18.3	19.9	3.6	>2

Figure 4. Calibration curves with R^2 values for **(a)** benzene, **(b)** o-xylene, **(c)** α-pinene and **(d)** β-caryophyllene in a gas cylinder (red) and in a custom liquid mixture (blue), delivered by the dynamic dilution system (Fig. 3). Normalized detector response on the y axis is the integrated area of the chromatographic peak divided by that of neohexane, our internal standard, on the same chromatogram. Maximum normalized detector response for a given compound ranged from 0.030 (β-caryophyllene, max concentration delivered 1.2 ppb) to 3.0 (o-xylene, max concentration delivered 12 ppb). Additionally, for benzene all data points had the mean of the 0 ppb values subtracted. Points are mean values of the individual samples at each level with error bars representing plus or minus 1 standard deviation. Dotted lines are best-fit lines forced through the origin, while R^2 values are from best fits not forced through the origin. Compounds show excellent linearity and agreement within 5 % between the gas cylinder and liquid solution.

8 ppb) or three (12 ppb) replicates at each level. From a separate gas cylinder, 1 ppm of neohexane was simultaneously sampled at a constant flow rate of 1 cm^3 min^{-1} and used to normalize the responses from the calibrant compounds. This step served to account for variations in sample volume and instrument sensitivity between samples.

Figure 4 shows calibration curves for benzene, o-xylene, α-pinene and β-caryophyllene from both the standard gas cylinder and the custom liquid solution evaporated and delivered via the dynamic dilution system. Normalized detector response on the y axis is the integrated area of the chromatographic peak divided by that of neohexane on the same chromatogram. Additionally, for benzene all data points had the mean of the 0 ppb values subtracted from them to account for a small persistent benzene contaminant likely due to the presence of Tenax TA in our adsorbent bed (Cao and Hewitt, 1994). Points are mean values of the six individual samples at each level (three samples at the highest level) with error bars representing plus or minus 1 standard deviation. To evaluate performance against our theoretical model of linear response with zero response at zero concentration, dotted curves are best-fit lines forced through the origin.

These compounds show excellent linearity with $R^2 \geq 0.93$. Agreement between gas and liquid is within 5 %, as measured by the difference in the slopes of the best-fit lines. The compounds span a range of volatility from that of a C_6 alkane to a C_{15} alkane, demonstrating the dynamic dilution system's suitability for evaporating and diluting IVOCs as well as VOCs.

Isoprene and methyl vinyl ketone were also analyzed and found to be linear, with $R^2 \geq 0.92$. However, we found consistently and significantly lower responses using the liquid mixtures, likely indicating issues during preparation and storage of the liquid solution related to the high volatility and reactivity of these compounds. For C_5 to C_6 alkane-equivalent-volatility compounds, we thus plan to continue to rely on

gas cylinder standards until and unless our liquid preparation process can be modified to remove this source of error.

Octamethylcyclotetrasiloxane and decamethylcyclopentasiloxane also had excellent linearity ($R^2 \geq 0.91$) but were found to have about 30 % higher responses using the liquid solution than using the gas cylinder. This could suggest depletion of these compounds in the gas cylinder, but we were not able to test this hypothesis.

3.3 Limits of detection

Limits of detection (LODs) are species dependent. On the I/VOC channel, limits of detection were estimated using the following formula:

$$\text{LOD} = 3 \cdot \sigma_{\text{blank}} / m, \qquad (1)$$

where σ_{blank} is the standard deviation of the integrated area of the chromatographic blank signal (12 replicates) of the quantification ion at the retention time of the analyte in question

Table 2. Limits of detection (LODs) for a selection of linear, branched and aromatic hydrocarbons on the I/VOC channel of cTAG. Compounds are presented in order of volatility from isopentane (5 carbon atoms) to dodecane (12 carbon atoms).

Compound	LOD (pptv)	Compound	LOD (pptv)	Compound	LOD (pptv)
Isopentane	2.0	2,3-Methylpentane	3.8	*o*-Xylene	3.7
1-Pentene	0.5	3-Methylhexane	0.6	Styrene	7.1
Pentane	2.2	Cyclohexane	0.9	Cumene	1.1
trans-2-Pentene	8.0	2,2,4-Trimethylpentane	0.9	*n*-Propylbenzene	2.5
cis-2-Pentene	1.3	Benzene	90*	Decane	2.7
Isoprene	6.7	Heptane	1.1	*m*- and *p*-Ethyltoluene	0.7
2,3-Dimethylbutane	2.3	Methylcyclohexane	1.1	1,3,5-Trimethylbenzene	1.5
2-Methylpentane	7.7	2,3,4-Trimethylpentane	1.3	*o*-Ethyltoluene	1.1
Cyclopentane	2.4	2-Methylheptane	1.2	1,2,4-Trimethylbenzene	0.6
3-Methylpentane	2.1	3-Methylheptane	0.9	1,2,3-Trimethylbenzene	0.9
1-Hexene	7.2	Octane	3.1	*m*-Diethylbenzene	0.6
Hexane	1.3	Toluene	60*	Undecane	2.6
2,4-Dimethylpentane	1.1	Nonane	2.8	*p*-Diethylbenzene	0.6
Methylcyclopentane	0.8	Ethylbenzene	3.9	Dodecane	2.4
2-Methylhexane	1.1	*m*- and *p*-Xylene	3.5		

* Contamination from the adsorbent materials used in the collector leads to elevated limits of detection for benzene and toluene, consistent with previous reports (Cao and Hewitt, 1994).

in units of counts, and m is the instrument sensitivity for that analyte, i.e., the slope of the best fit to the calibration curve, in units of counts pptv^{-1} (Foley and Dorsey, 1984).

Limits of detection were estimated for the 44 compounds present in the Photochemical Assessment Monitoring Stations 57-component commercial standard (Scott-Specialty) that are within the volatility range collected on cTAG's I/VOC channel, including linear, branched and aromatic hydrocarbons (Table 2). The LODs range from 0.5 to 8 pptv except for benzene and toluene, which have known contamination issues from the Tenax used in the collector (Cao and Hewitt, 1994).

The SVOC channel is equivalent to one channel of the SV-TAG as described in Isaacman et al. (2014). The average limit of detection reported for that instrument is 1 to 2 ng m^{-3} (~ 0.1 ppt) for a 20 min sample collected at 10 L min^{-1}. We determined that the LOD for the SVOC channel on cTAG determined according to Eq. (1) is consistent with that reported previously for SV-TAG.

### 3.4 Evaluation of ozone removal on the I/VOC channel

Ozone has been shown to be able to penetrate standard VOC sampling inlets and react with certain analytes collected on adsorbent beds like ours (Calogirou et al., 1996; Helmig, 1997; Pollmann et al., 2005). A common practice for ozone removal is to pass the sample flow through a sodium-thiosulfate-impregnated filter upstream of the adsorbent bed (Helmig, 1997). Pollmann et al. (2005) demonstrated that this technique is effective at preventing ozone reaction artifacts for some sesquiterpenes as well as the previously studied monoterpenes and other hydrocarbons. We explored the effects of ozone on the recovery of a suite of compounds of

interest known to have short lifetimes with respect to reaction with ozone, including monoterpenes and sesquiterpenes, and tested how placement of filters impregnated with sodium thiosulfate (Na$_2$S$_2$O$_3$) upstream of the collector altered the recovery of these compounds. The Na$_2$S$_2$O$_3$ filters were obtained from the Barsanti research group at UC Riverside (Hatch et al., 2017).

To quantify the effects of the presence of ozone in sampled air, we diluted air from the output of an ozone generator (model 1008-RS, Dasibi Environmental Corp) with humidified zero air to achieve an ozone concentration of 100 ppb ozone. We then verified that the ozone was completely removed by three inline filters by measuring the ozone concentration downstream (model 202, 2B Technologies). At 1 L min^{-1} (20 times our ambient sampling rate), ozone breakthrough through a stack of three Na$_2$S$_2$O$_3$ filters occurred after 8 h, indicating a single filter stack can be used without breakthrough for 9600 min, or about 20 d of continuous operation.

After verifying the efficient removal of ozone by the filter stack, we combined 9 L min^{-1} of 100 ppb ozone with the 1 L min^{-1} output from our dynamic dilution calibration system described in Sect. 2.5. Using that calibration system, we evaporated a liquid mixture of sesquiterpenes and other compounds to achieve a concentration of 5.60 ppb, which once combined with the 9 L min^{-1} zero air was reduced to 560 ppt for sampling.

We sampled this liquid mixture onto the I/VOC channel under four different conditions: without ozone and without a Na$_2$S$_2$O$_3$ filter, without ozone and with the filter, with 100 ppb ozone and without the filter, and with 100 ppb ozone with the filter. This allowed us to establish (1) whether an

Instrument Response With and Without Na$_2$S$_2$O$_3$ Filter In Presence or Absence of O$_3$
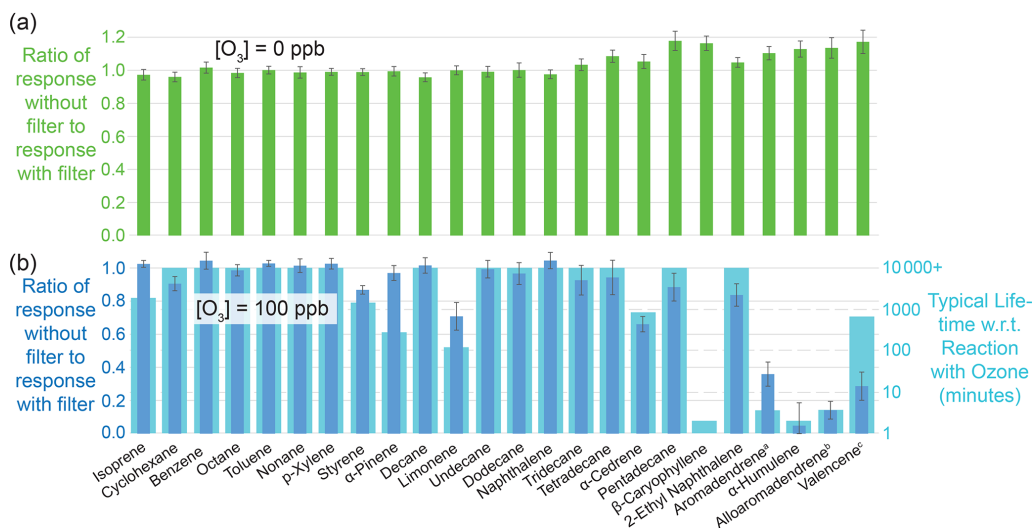
Figure 5. Results of evaluation of effectiveness of sodium thiosulfate filter in mitigating the effects of ozone on reactive analytes during collection of VOCs and IVOCs. Error bars represent plus or minus 1 standard deviation of six replicate measurements. Panel **(a)** confirms that in the absence of ozone, the filter does not affect the detected quantities of each compound, except for slight (< 15 %) losses of IVOCs with the filter present, leading to response ratios greater than 1. Panel **(b)** demonstrates that the filter prevents substantial losses of reactive species in the presence of ozone, confirming that without preventive measures ozone can significantly deplete certain analytes. Values are compared with published lifetimes with respect to reaction with ozone, with overall qualitative agreement. Published lifetimes are from Atkinson and Arey (2003) unless above 10 000 min or otherwise indicated. **(a)** Pollmann et al. (2005). **(b)** No published experimental value, assumed reactivity equal to that of the stereoisomer aromadendrene. **(c)** Ham (2013).

ozone removal method is needed in our instrument for accurate quantification of ozone-reactive species such as some sesquiterpenes and (2) whether the presence of the filter altered the concentrations of non-ozone-reactive VOCs and IVOCs or of reactive VOCs and IVOCs in the absence of ozone.

Figure 5 shows the effects of the Na$_2$S$_2$O$_3$ filter on several analytes of interest with and without ozone. In the absence of ozone, VOC and IVOC concentrations were unperturbed by the presence of the filter except for manageable losses of lower-volatility compounds when the filter was present (Fig. 5a). In the presence of ozone, placement of the Na$_2$S$_2$O$_3$-impregnated filters in the sampling flow upstream of the collector prevented degradation (Fig. 5b). In general, losses of analytes in the absence of the filter were greater for compounds with lower atmospheric lifetimes with respect to reaction with ozone.

The results imply having a Na$_2$S$_2$O$_3$-impregnated filter in-line improves quantification of ozone-reactive species without significant downsides. However, prior literature suggests some very polar compounds, not tested in this experiment, may become trapped on the filter, hindering their measurement (Hatch et al., 2017). Such compounds are unlikely to elute on our GC column, which is optimized for less-polar species. During normal operation of the instrument, we thus include a filter inline.

3.5 Region of sensitivity overlap

Some of the chemical compounds with alkane-equivalent volatility between that of *n*-tetradecane and *n*-hexadecane can be detected and quantified on both the I/VOC and the SVOC channels. Comparing quantifications of such compounds between channels can serve as a useful check of instrument performance. However in practice the number of compounds suitable for such an analysis is small, and for any given ambient data set there may be none. One reason for this is the 200-times-larger sample volume collected on the SVOC channel, so that some compounds that are easily quantifiable on the SVOC channel are below detection limit on the I/VOC channel. Compounds which are reactive with ozone on timescales of under an hour or so, including many sesquiterpenes (Fig. 5), must be quantified on the I/VOC channel where ozone is removed at the inlet. Highly polar species may not elute on the I/VOC column; the SVOC channel with its online derivatization is more appropriate in this case. Thus there is usually reason to choose one channel over the other for quantification purposes.

A survey of compounds from the ambient data set from the cTAG deployment in McCall, Idaho, for the 2019 Fire Influence on Regional to Global Environments and Air Quality (FIREX-AQ) field campaign was conducted to test cross-channel agreement for compounds in the volatility overlap
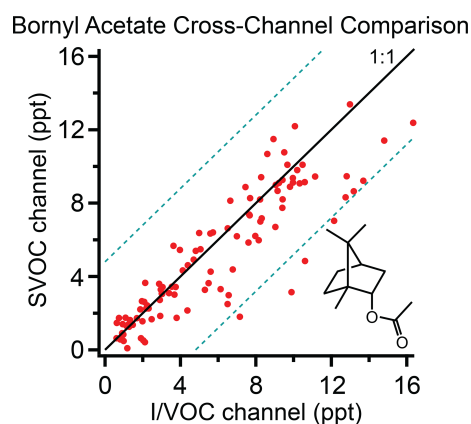
Figure 6. Bornyl acetate measured on the I/VOC and SVOC channels of cTAG during FIREX-AQ. Dashed lines represent ± 4.8 ppt (3 times the I/VOC channel limit of detection for bornyl acetate). A total of 96 % of data points fall within the region bounded by the dashed lines. R^2 is 0.79.

region. Of the compounds found, all but one, bornyl acetate, were subject to one of the restrictions listed above.

Bornyl acetate ($C_{12}H_{20}O_2$) is found in essential oils from pine trees (Garneau et al., 2012). Though it elutes close to tridecane, which is outside the reliably quantifiable range on the SVOC channel, we were able to quantify it on both the I/VOC and SVOC channels in McCall, Idaho, during the 2019 FIREX-AQ field campaign. The concentration ranges from 0.1 to 16.5 ppt as measured on the SVOC channel. The correlation of concurrent sampling points on both channels is shown in Fig. 6. The I/VOC and SVOC channels agree on average within 11 %, with $R^2 = 0.79$ and 96 % of the data points agreeing within ± 4.8 ppt (3 times the I/VOC channel limit of detection for bornyl acetate). We consider this excellent agreement between the two channels given that the sample sizes differ by more than 2 orders of magnitude, they are calibrated independently and all data points are within a factor of 10 of the detection limit on the I/VOC channel.

3.6 Measurements of ambient air

The cTAG was deployed in Livermore, CA in April 2018 for its first field test. This test was undertaken to evaluate the stability of instrument performance during round-the-clock automated operation and demonstrate the capability to measure concentrations of a variety of compound classes from C_5 to C_{32} alkane-equivalent volatility. The instrument was deployed approximately 100 m from a Bay Area Air Quality Management District monitoring site to make use of their air quality measurements for comparison (specifically, ozone and ambient temperature reported here). Livermore is a valley city on the eastern and downwind edge of the San Francisco Bay Area, where pollution outflow from the region combined with optimal conditions for secondary photochemical smog formation frequently leads to the highest ozone
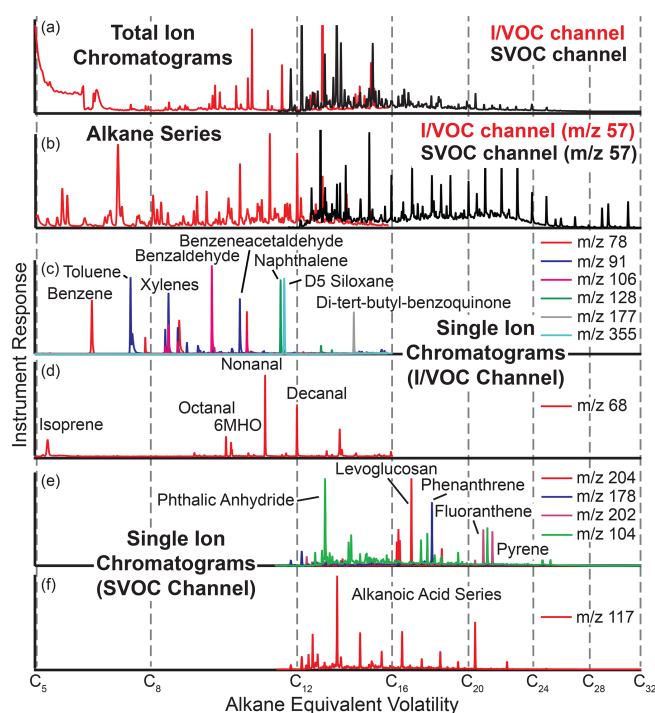

Figure 7. Example chromatograms from cTAG. Panels **(a)** and **(b)** from FIREX-AQ 2019 in McCall, Idaho, demonstrate the range of volatility covered by the two channels, including their overlap region. Single ion chromatograms (panels **c**, **d** and **f** from Berkeley, California, and **e** from Livermore, California) show examples of the compound classes observable by cTAG, including aromatics, polycyclic aromatic hydrocarbons, organic acids and anhydrosugars.
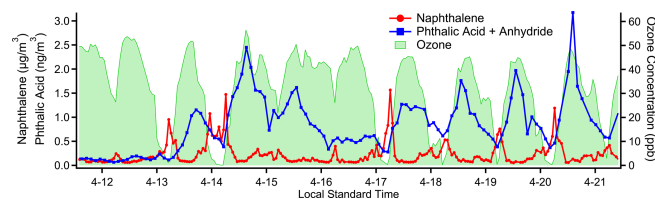
Figure 8. Concentration timelines for naphthalene, a primary emission from vehicle exhaust measured on cTAG's I/VOC channel, and the sum of phthalic anhydride and phthalic acid, secondary photooxidation products of naphthalene detected on cTAG's SVOC channel. Another secondary compound, ozone, measured at a nearby Bay Area Air Quality Management District monitoring site, provides an independent indication of photochemical activity.

levels in the Bay Area (Knoderer et al., 2018). In addition, Livermore has substantial wood burning for heat during winter. An analysis of a subset of VOCs, IVOCs and SVOCs measured in Livermore by cTAG is presented to demonstrate some of the analytical capabilities of this instrument.

cTAG is sensitive to a wide variety of organic compound classes. Figure 7 shows some sample chromatograms from Berkeley, California; ambient air sampled from outside the lab window; the Livermore 2018 deployment; and McCall,
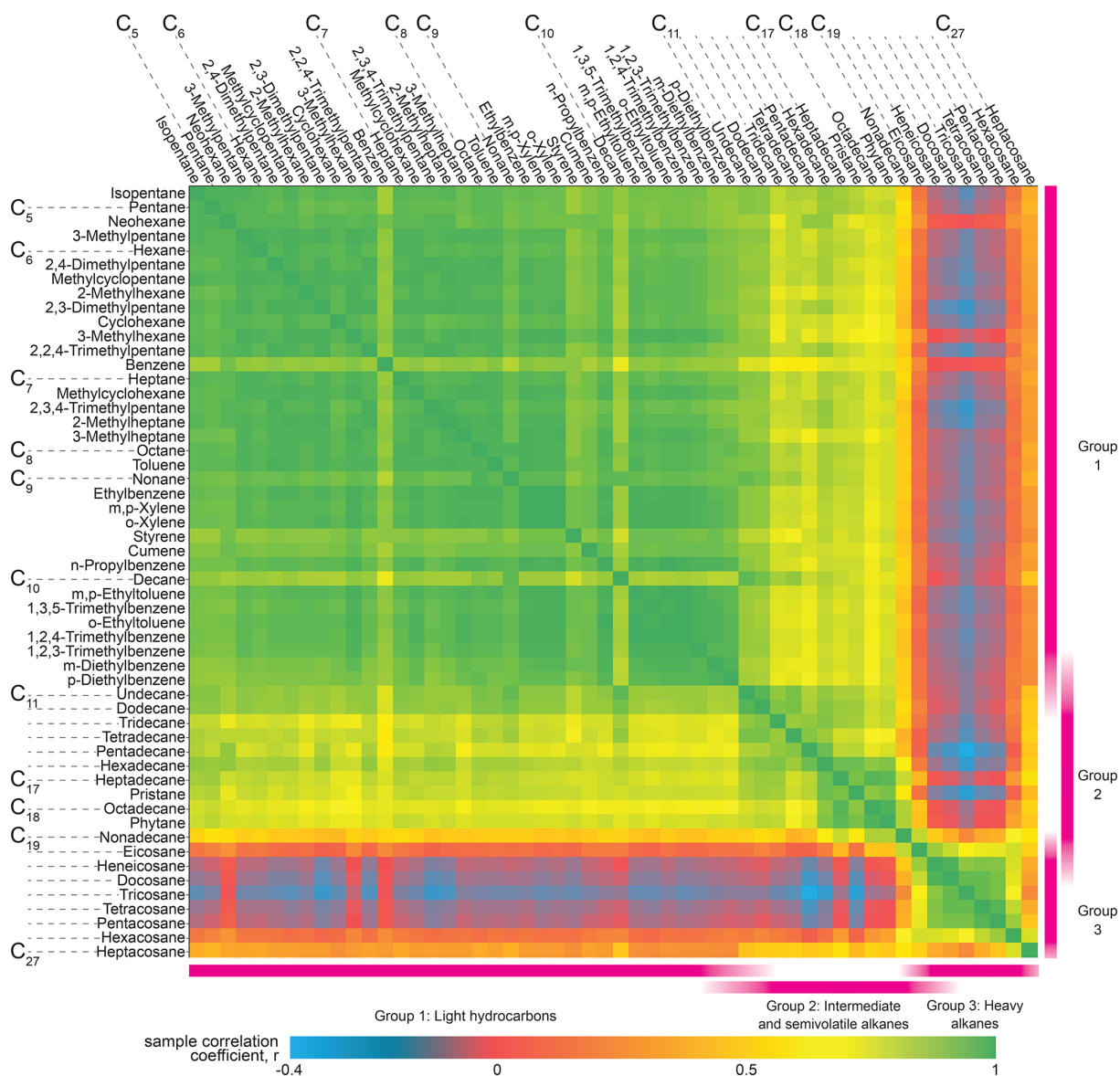
Figure 9. Pearson's *R* correlation matrix for a suite of petroleum-derived compounds observed by cTAG in Livermore, California, between 11 April and 21 April 2018, ordered by volatility. Two distinct groupings emerge from C_5 alkane-equivalent volatility to about C_{11} and C_{20} to C_{26}, with a third less distinct but still prominent grouping from approximately C_{11} to C_{19}.

Idaho, for the 2019 FIREX-AQ field campaign highlighting compounds of interest. The total ion chromatograms and selected ion chromatograms with a mass-to-charge ratio of 57, the dominant ion in most alkanes, show the volatility range detected as well as the overlap region of both channels between C_{14} and C_{16} alkane-equivalent volatility. Common air toxics such as benzene, toluene, ethylbenzene, xylene, polycyclic aromatic hydrocarbons and quinones are readily visible, as well as biogenic terpenes and aldehydes, organic acids and polar biomass burning markers. Compounds as polar as glucose (five hydroxy groups) can be detected on the SVOC channel.

cTAG can observe gas-phase chemicals and many of their oxidation products in gas and particle phases. Naphthalene is a gas-phase product of incomplete combustion of fossil fuels (Baek et al., 1991) and in urban areas has been observed to primarily originate from vehicle emissions (Howsam and Jones, 1998; Lim et al., 1999). Phthalic anhydride is a major gas-phase photooxidation product of naphthalene, and phthalic acid has been found in secondary organic aerosol formed from naphthalene photooxidation (Chan et al., 2009; Kleindienst et al., 2012; Wang et al., 2007). cTAG is sensitive to naphthalene on the I/VOC channel and the sum of phthalic anhydride and phthalic acid on the SVOC channel.
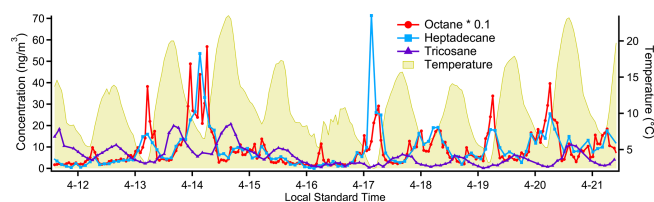
Figure 10. Timelines for characteristic species from each of the three main groupings of compounds evident in the correlation matrix (Fig. 9). The two more volatile groups, represented by octane and heptadecane, tend to peak in the early morning, consistent with morning-rush-hour cold-start emissions. The least-volatile group, which includes tricosane, appears to have an evaporative source as it tracks closely, but slightly delayed, with ambient temperature.

(We have found through laboratory testing of an authentic phthalic acid standard that phthalic acid converts to and is detected as phthalic anhydride in cTAG.) As Fig. 8 shows, the precursor and products have extremely distinct temporal profiles, with naphthalene concentrations elevated at night and in the early morning hours while the phthalic anhydride plus phthalic acid signal rises in the early to mid-afternoon, consistent with secondary formation and in agreement with observations at other field sites (Williams et al., 2010).

An analysis of straight-chain alkanes along with some aromatics, alkenes and branched alkanes demonstrates cTAG's volatility range and highlights the different source categories for sub-groups of this set of compounds. The cross-correlation matrix (Fig. 9) indicates three distinct groupings of compounds. The first group is characteristic of gasoline emissions, spanning a volatility range from below C_5 alkane-equivalent volatility to about C_{11} (Gentner et al., 2013) and including linear, branched and cyclic alkanes as well as aromatics. It shows short periods of elevated levels in the early morning consistent with a morning rush hour traffic pattern (Fig. 10). The lack of a similar peak near the end of the day could point to the outsized contribution of cold-start emissions to total VOC emissions from gasoline vehicles (Drozd et al., 2016, 2019), as the sampling site was located in a primarily residential area. There is also a well-defined group from C_{20} to C_{26} alkanes with a smooth diurnal variability and daily maximum concentration in the late afternoon (Fig. 10), consistent with a petroleum-based evaporative source such as asphalt (Khare et al., 2020). The afternoon peaks in concentration result in a clear anti-correlation with the rest of the alkanes in Fig. 9 (blue and dark red areas). The third group is less pronounced but follows a roughly similar pattern to the high-volatility source category and likely corresponds to diesel fuel emissions, which typically span a volatility range from about C_{10} to C_{22}, with minor contributions from C_{23}–C_{25} alkanes (Gentner et al., 2013; Isaacman et al., 2012; Drozd et al., 2021). Our data suggest that overlapping contributions from gasoline and the petroleum-based evaporative sources make this source group less well-defined in the corre-

lation matrix, but semivolatile compounds that have no other major source still correlate well with each other.

4 Summary and concluding remarks

The Comprehensive Thermal Desorption Aerosol Gas Chromatograph is a novel instrument capable of measuring non-polar and some polar organic compounds as well as some more oxidized semivolatile organics from C_5 through C_{32} alkane-equivalent volatility on two separate channels connected to a single HRToFMS. This set of quantifiable compounds encompasses many key VOC pollutants, reactive intermediates, and secondary products, all captured at hourly time resolution. The expanded range of measurable compounds allows for more robust source categorization, with detailed chemical specificity of each identified source category.

Building off development of previous TAG family instruments, development for cTAG focused on the I/VOC channel as well as miniature gas chromatographs to enhance field portability of the instrument. The I/VOC collector is optimized for collection of C_5 through C_{16} alkane-equivalent-volatility organics to capture major biogenic VOC and IVOC emissions and ensure overlap with the SVOC channel collection range. The dynamic dilution system with controlled liquid evaporation developed in house is shown to produce stable, linear calibration curves and allows for maximum flexibility in calibration of the I/VOC channel, including quantification of commercially available VOCs and IVOCs not commonly available in calibration gas cylinders or which are difficult or prohibitively expensive to put in such cylinders. Placement of a $Na_2S_2O_3$-impregnated filter in the sampling path for the I/VOC channel is shown to effectively remove ozone without removing appreciable amounts of analytes of interest. Example chromatograms, timelines and correlations for a suite of compounds at a polluted urban field site demonstrate some of the potential for analysis of the data sets produced by this instrument.

Comprehensive, speciated measurements of reactive organic carbon across the full range of volatility are required to fully understand the atmospheric processes that lead to secondary aerosol formation and dictate the atmospheric lifetimes of key atmospheric oxidants (Heald and Kroll, 2020; Hunter et al., 2017). Moreover, the organic composition and thus the dominant atmospheric processes are likely to vary greatly in different environments (e.g., remote, forested, rural/agricultural, urban), and current science lacks such comprehensive measurements across these different types of sites (Heald and Kroll, 2020). The cTAG is designed for field portability and speciated measurement of a significant fraction of the total reactive organic carbon, making it an ideal choice for helping to close this gap in our current scientific understanding.

Appendix A: Miniature gas chromatogram development

cTAG uses dual miniature gas chromatographs to preserve compactness and independent temperature control. Figure A1 shows a schematic of the final design and a photo of a GC hub on the instrument. Having reproducible temperature ramps is critical for batch chromatogram analysis, since the exact elution time of each compound is dependent upon the column temperature. Figure A2 shows that we can run a consistent, repeatable temperature program using PID control on the mini GCs.
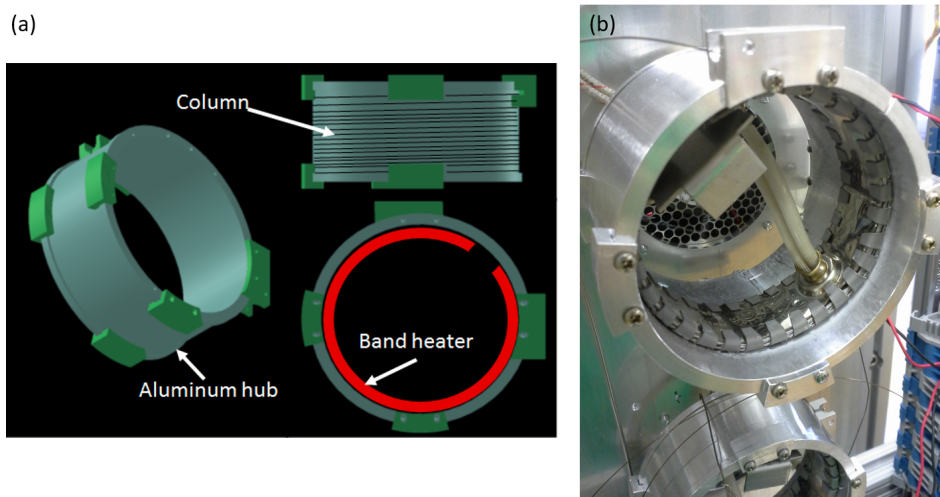
Figure A1. Schematic and photo of miniature gas chromatographs. Clamps on the edges of the rim of the hub hold the chromatography column in place at each end. An aluminum sheet is wrapped around the outside of the hub over the column to further ensure even heating of the column itself.
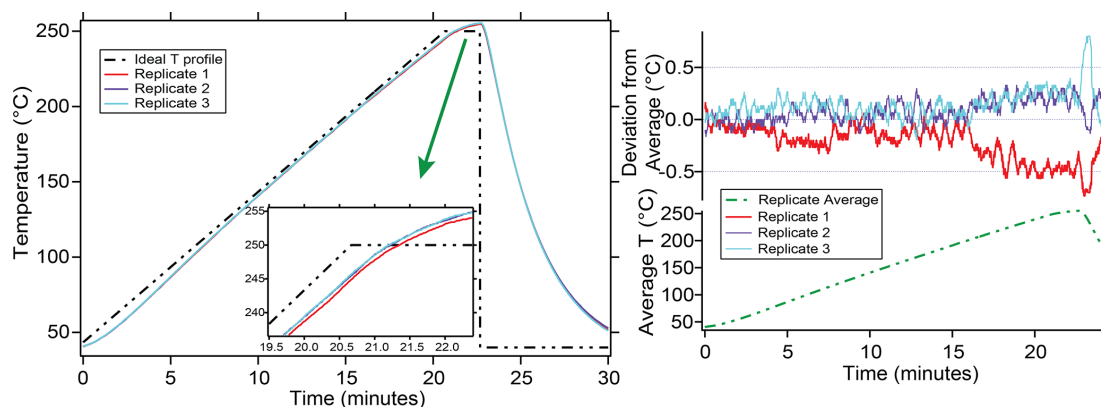
Figure A2. Demonstration of reproducibility of temperature ramps on the miniature gas chromatographs. This leads to consistent elution times of compounds of interest, streamlining batch peak integration.

References

Atkinson, R. and Arey, J.: Atmospheric Degradation of Volatile Organic Compounds, Chem. Rev., 103, 4605–4638, https://doi.org/10.1021/cr0206420, 2003.

Baek, S. O., Field, R. A., Goldstone, M. E., Kirk, P. W., Lester, J. N., and Perry, R.: A review of atmospheric polycyclic aromatic hydrocarbons: Sources, fate and behavior, Water Air Soil Pollut., 60, 279–300, https://doi.org/10.1007/BF00282628, 1991.

Bouvier-Brown, N. C., Goldstein, A. H., Gilman, J. B., Kuster, W. C., and de Gouw, J. A.: In-situ ambient quantification of monoterpenes, sesquiterpenes, and related oxygenated compounds during BEARPEX 2007: implications for gas- and particle-phase chemistry, Atmos. Chem. Phys., 9, 5505–5518, https://doi.org/10.5194/acp-9-5505-2009, 2009.

Calogirou, A., Larsen, B. R., Brussol, C., Duane, M., and Kotzias, D.: Decomposition of Terpenes by Ozone during Sampling on Tenax, Anal. Chem., 68, 1499–1506, https://doi.org/10.1021/ac950803i, 1996.

Cao, X.-L. and Hewitt, C. N.: Build-up of artifacts on adsorbents during storage and its effect on passive sampling and gas chromatography-flame ionization detection of low concentrations of volatile organic compounds in air, J. Chromatogr. A, 688, 368–374, https://doi.org/10.1016/0021-9673(94)00908-2, 1994.

Chan, A. W. H., Kautzman, K. E., Chhabra, P. S., Surratt, J. D., Chan, M. N., Crounse, J. D., Kürten, A., Wennberg, P. O., Flagan, R. C., and Seinfeld, J. H.: Secondary organic aerosol formation from photooxidation of naphthalene and alkylnaphthalenes: implications for oxidation of intermediate volatility organic compounds (IVOCs), Atmos. Chem. Phys., 9, 3049–3060, https://doi.org/10.5194/acp-9-3049-2009, 2009.

Chan, A. W. H., Kreisberg, N. M., Hohaus, T., Campuzano-Jost, P., Zhao, Y., Day, D. A., Kaser, L., Karl, T., Hansel, A., Teng, A. P., Ruehl, C. R., Sueper, D. T., Jayne, J. T., Worsnop, D. R., Jimenez, J. L., Hering, S. V., and Goldstein, A. H.: Speciated measurements of semivolatile and intermediate volatility organic compounds (S/IVOCs) in a pine forest during BEACHON-RoMBAS 2011, Atmos. Chem. Phys., 16, 1187–1205, https://doi.org/10.5194/acp-16-1187-2016, 2016.

Chung, M. Y., Maris, C., Krischke, U., Meller, R., and Paulson, S. E.: An investigation of the relationship between total nonmethane organic carbon and the sum of speciated hydrocarbons and carbonyls measured by standard GC/FID: measurements in the Los Angeles air basin, Atmos. Environ., 37, 159–170, https://doi.org/10.1016/S1352-2310(03)00388-1, 2003.

Column/Fan Modules for Fast GC: https://www.vici.com/gc/column-fan-modules.php, last access: 6 October 2020.

Cropper, P. M., Overson, D. K., Cary, R. A., Eatough, D. J., Chow, J. C., and Hansen, J. C.: Development of the GC-MS organic aerosol monitor (GC-MS OAM) for in-field detection of particulate organic compounds, Atmos. Environ., 169, 258–266, https://doi.org/10.1016/j.atmosenv.2017.09.019, 2017.

Definition of Breakthrough Volumes: https://www.sisweb.com/index/referenc/resin3.htm, last access: 29 September 2020.

de Gouw, J. A., Middlebrook, A. M., Warneke, C., Ahmadov, R., Atlas, E. L., Bahreini, R., Blake, D. R., Brock, C. A., Brioude, J., Fahey, D. W., Fehsenfeld, F. C., Holloway, J. S., Le Henaff, M., Lueb, R. A., McKeen, S. A., Meagher, J. F., Murphy, D. M., Paris, C., Parrish, D. D., Perring, A. E., Pollack, I. B., Ravishankara, A. R., Robinson, A. L., Ryer-

son, T. B., Schwarz, J. P., Spackman, J. R., Srinivasan, A., and Watts, L. A.: Organic aerosol formation downwind from the Deepwater Horizon oil spill, Science, 331, 1295–1299, https://doi.org/10.1126/science.1200320, 2011.

Docherty, K. S., Stone, E. A., Ulbrich, I. M., DeCarlo, P. F., Snyder, D. C., Schauer, J. J., Peltier, R. E., Weber, R. J., Murphy, S. M., Seinfeld, J. H., Grover, B. D., Eatough, D. J., and Jimenez, J. L.: Apportionment of Primary and Secondary Organic Aerosols in Southern California during the 2005 Study of Organic Aerosols in Riverside (SOAR-1), Environ. Sci. Technol., 42, 7655–7662, https://doi.org/10.1021/es8008166, 2008.

Drozd, G. T., Zhao, Y., Saliba, G., Frodin, B., Maddox, C., Weber, R. J., Chang, M.-C. O., Maldonado, H., Sardar, S., Robinson, A. L., and Goldstein, A. H.: Time Resolved Measurements of Speciated Tailpipe Emissions from Motor Vehicles: Trends with Emission Control Technology, Cold Start Effects, and Speciation, Environ. Sci. Technol., 50, 13592–13599, https://doi.org/10.1021/acs.est.6b04513, 2016.

Drozd, G. T., Zhao, Y., Saliba, G., Frodin, B., Maddox, C., Oliver Chang, M.-C., Maldonado, H., Sardar, S., Weber, R. J., Robinson, A. L., and Goldstein, A. H.: Detailed Speciation of Intermediate Volatility and Semivolatile Organic Compound Emissions from Gasoline Vehicles: Effects of Cold-Starts and Implications for Secondary Organic Aerosol Formation, Environ. Sci. Technol., 53, 1706–1714, https://doi.org/10.1021/acs.est.8b05600, 2019.

Drozd, G. T., Weber, R. J., and Goldstein, A. H.: Highly Resolved Composition during Diesel Evaporation with Modeled Ozone and Secondary Aerosol Formation: Insights into Pollutant Formation from Evaporative Intermediate Volatility Organic Compound Sources, Environ. Sci. Technol., 55, 5742–5751, https://doi.org/10.1021/acs.est.0c08832, 2021.

Engel, A., Rigby, M., Burkholder, J. B., Fernandez, R. P., Froidevaux, L., Hall, B. D., Hossaini, R., Saito, T., Vollmer, M. K., and Yao, B.: Update on Ozone-Depleting Substances (ODSs) and Other Gases of Interest to the Montreal Protocol, chap. 1, in: Scientific Assessment of Ozone Depletion: 2018, Global Ozone Research and Monitoring Project – Report No. 58, World Meteorological Organization, Geneva, Switzerland, 2018.

Ervens, B., Turpin, B. J., and Weber, R. J.: Secondary organic aerosol formation in cloud droplets and aqueous particles (aqSOA): a review of laboratory, field and model studies, Atmos. Chem. Phys., 11, 11069–11102, https://doi.org/10.5194/acp-11-11069-2011, 2011.

Foley, J. P. and Dorsey, J. G.: Clarification of the limit of detection in chromatography, Chromatographia, 18, 503-511, https://doi.org/10.1007/BF02267236, 1984.

Garneau, F.-X., Collin, G., Gagnon, H., and Pichette, A.: Chemical Composition of the Hydrosol and the Essential Oil of Three Different Species of the Pinaceae Family: Picea glauca (Moench) Voss, Picea mariana (Mill.) B.S.P., and Abies balsamea (L.) Mill., J. Essent. Oil Bear. Pl., 15, 227–236, https://doi.org/10.1080/0972060X.2012.10644040, 2012.

Gentner, D. R., Isaacman, G., Worton, D. R., Chan, A. W. H., Dallmann, T. R., Davis, L., Liu, S., Day, D. A., Russell, L. M., Wilson, K. R., Weber, R., Guha, A., Harley, R. A., and Goldstein, A. H.: Elucidating secondary organic aerosol from diesel and gasoline vehicles through detailed characterization of organic

carbon emissions, P. Natl. Acad. Sci. USA, 109, 18318–18323, https://doi.org/10.1073/pnas.1212272109, 2012.

Gentner, D. R., Worton, D. R., Isaacman, G., Davis, L. C., Dallmann, T. R., Wood, E. C., Herndon, S. C., Goldstein, A. H., and Harley, R. A.: Chemical Composition of Gas-Phase Organic Carbon Emissions from Motor Vehicles and Implications for Ozone Production, Environ. Sci. Technol., 47, 11837–11848, https://doi.org/10.1021/es401470e, 2013.

Goldan, P. D., Kuster, W. C., Williams, E., Murphy, P. C., Fehsenfeld, F. C., and Meagher, J.: Nonmethane hydrocarbon and oxy hydrocarbon measurements during the 2002 New England Air Quality Study, J. Geophys. Res.-Atmos., 109, 1–14, https://doi.org/10.1029/2003JD004455, 2004.

Goldstein, A. H. and Galbally, I. E.: Known and Unexplored Organic Constituents in the Earth's Atmosphere, Environ. Sci. Technol., 41, 1514–1521, https://doi.org/10.1021/es072476p, 2007.

Goldstein, A. H., Daube, B. C., Munger, J. W., and Wofsy, S. C.: Automated in-situ monitoring of atmospheric non-methane hydrocarbon concentrations and gradients, J. Atmos. Chem., 21, 43–59, https://doi.org/10.1007/BF00712437, 1995.

Hallquist, M., Wenger, J. C., Baltensperger, U., Rudich, Y., Simpson, D., Claeys, M., Dommen, J., Donahue, N. M., George, C., Goldstein, A. H., Hamilton, J. F., Herrmann, H., Hoffmann, T., Iinuma, Y., Jang, M., Jenkin, M. E., Jimenez, J. L., Kiendler-Scharr, A., Maenhaut, W., McFiggans, G., Mentel, Th. F., Monod, A., Prévôt, A. S. H., Seinfeld, J. H., Surratt, J. D., Szmigielski, R., and Wildt, J.: The formation, properties and impact of secondary organic aerosol: current and emerging issues, Atmos. Chem. Phys., 9, 5155–5236, https://doi.org/10.5194/acp-9-5155-2009, 2009.

Ham, J. E.: Rate Constants for the Gas-Phase Reactions of Ozone and Nitrate Radicals with the Sesquiterpenes: Valencene and Farnesol: Gas-Phase Reactions of Ozone and Nitrate Radicals with the Sesquiterpenes, Int. J. Chem. Kinet., 45, 508–514, https://doi.org/10.1002/kin.20789, 2013.

Hatch, L. E., Yokelson, R. J., Stockwell, C. E., Veres, P. R., Simpson, I. J., Blake, D. R., Orlando, J. J., and Barsanti, K. C.: Multi-instrument comparison and compilation of non-methane organic gas emissions from biomass burning and implications for smoke-derived secondary organic aerosol precursors, Atmos. Chem. Phys., 17, 1471–1489, https://doi.org/10.5194/acp-17-1471-2017, 2017.

Heald, C. L. and Kroll, J. H.: The fuel of atmospheric chemistry: Toward a complete description of reactive organic carbon, Sci. Adv., 6, eaay8967, https://doi.org/10.1126/sciadv.aay8967, 2020.

Helmig, D.: Ozone removal techniques in the sampling of atmospheric volatile organic trace gases, Atmos. Environ., 31, 3635–3651, https://doi.org/10.1016/S1352-2310(97)00144-1, 1997.

Hopkins, J. R., Lewis, A. C., and Read, K. A.: A two-column method for long-term monitoring of non-methane hydrocarbons (NMHCs) and oxygenated volatile organic compounds (o-VOCs), J. Environ. Monit., 5, 8–13, https://doi.org/10.1039/B202798D, 2003.

Howsam, M. and Jones, K. C.: Sources of PAHs in the Environment, in: PAHs and Related Compounds: Chemistry, edited by: Neilson, A. H., Springer, Berlin, Heidelberg, 137–174, https://doi.org/10.1007/978-3-540-49697-7_4, 1998.

Hunter, J. F., Day, D. A., Palm, B. B., Yatavelli, R. L. N., Chan, A. W. H., Kaser, L., Cappellin, L., Hayes, P. L., Cross, E. S., Carrasquillo, A. J., Campuzano-Jost, P., Stark, H., Zhao, Y., Hohaus, T., Smith, J. N., Hansel, A., Karl, T., Goldstein, A. H., Guenther, A., Worsnop, D. R., Thornton, J. A., Heald, C. L., Jimenez, J. L., and Kroll, J. H.: Comprehensive characterization of atmospheric organic carbon at a forested site, Nat. Geosci., 10, 748–753, https://doi.org/10.1038/ngeo3018, 2017.

Isaacman, G., Kreisberg, N. M., Worton, D. R., Hering, S. V., and Goldstein, A. H.: A versatile and reproducible automatic injection system for liquid standard introduction: application to in-situ calibration, Atmos. Meas. Tech., 4, 1937–1942, https://doi.org/10.5194/amt-4-1937-2011, 2011.

Isaacman, G., Wilson, K. R., Chan, A. W. H., Worton, D. R., Kimmel, J. R., Nah, T., Hohaus, T., Gonin, M., Kroll, J. H., Worsnop, D. R., and Goldstein, A. H.: Improved Resolution of Hydrocarbon Structures and Constitutional Isomers in Complex Mixtures Using Gas Chromatography-Vacuum Ultraviolet-Mass Spectrometry, Anal. Chem., 84, 2335–2342, https://doi.org/10.1021/ac2030464, 2012.

Isaacman, G., Kreisberg, N. M., Yee, L. D., Worton, D. R., Chan, A. W. H., Moss, J. A., Hering, S. V., and Goldstein, A. H.: Online derivatization for hourly measurements of gas- and particle-phase semi-volatile oxygenated organic compounds by thermal desorption aerosol gas chromatography (SV-TAG), Atmos. Meas. Tech., 7, 4417–4429, https://doi.org/10.5194/amt-7-4417-2014, 2014.

Isaacman-VanWertz, G., Sueper, D. T., Aikin, K. C., Lerner, B. M., Gilman, J. B., de Gouw, J. A., Worsnop, D. R., and Goldstein, A. H.: Automated single-ion peak fitting as an efficient approach for analyzing complex chromatographic data, J. Chromatogr. A, 1529, 81–92, https://doi.org/10.1016/j.chroma.2017.11.005, 2017.

Isaacman-VanWertz, G., Massoli, P., O'Brien, R., Lim, C., Franklin, J. P., Moss, J. A., Hunter, J. F., Nowak, J. B., Canagaratna, M. R., Misztal, P. K., Arata, C., Roscioli, J. R., Herndon, S. T., Onasch, T. B., Lambe, A. T., Jayne, J. T., Su, L., Knopf, D. A., Goldstein, A. H., Worsnop, D. R., and Kroll, J. H.: Chemical evolution of atmospheric organic carbon over multiple generations of oxidation, Nat. Chem., 10, 462–468, https://doi.org/10.1038/s41557-018-0002-2, 2018.

Jardine, K. J., Henderson, W. M., Huxman, T. E., and Abrell, L.: Dynamic Solution Injection: a new method for preparing pptv–ppbv standard atmospheres of volatile organic compounds, Atmos. Meas. Tech., 3, 1569–1576, https://doi.org/10.5194/amt-3-1569-2010, 2010.

Jimenez, J. L., Canagaratna, M. R., Donahue, N. M., Prevot, A. S. H., Zhang, Q., Kroll, J. H., DeCarlo, P. F., Allan, J. D., Coe, H., Ng, N. L., Aiken, A. C., Docherty, K. S., Ulbrich, I. M., Grieshop, A. P., Robinson, A. L., Duplissy, J., Smith, J. D., Wilson, K. R., Lanz, V. A., Hueglin, C., Sun, Y. L., Tian, J., Laaksonen, A., Raatikainen, T., Rautiainen, J., Vaattovaara, P., Ehn, M., Kulmala, M., Tomlinson, J. M., Collins, D. R., Cubison, M. J., E, Dunlea, J., Huffman, J. A., Onasch, T. B., Alfarra, M. R., Williams, P. I., Bower, K., Kondo, Y., Schneider, J., Drewnick, F., Borrmann, S., Weimer, S., Demerjian, K., Salcedo, D., Cottrell, L., Griffin, R., Takami, A., Miyoshi, T., Hatakeyama, S., Shimono, A., Sun, J. Y., Zhang, Y. M., Dzepina, K., Kimmel, J. R., Sueper, D., Jayne, J. T., Herndon, S. C., Trimborn, A.

M., Williams, L. R., Wood, E. C., Middlebrook, A. M., Kolb, C. E., Baltensperger, U., and Worsnop, D. R.: Evolution of Organic Aerosols in the Atmosphere, Science, 326, 1525–1529, https://doi.org/10.1126/science.1180353, 2009.

Karbiwnyk, C. M., Mills, C. S., Helmig, D., and Birks, J. W.: Use of Chlorofluorocarbons as Internal Standards for the Measurement of Atmospheric Non-Methane Volatile Organic Compounds Sampled onto Solid Adsorbent Cartridges, Environ. Sci. Technol., 37, 1002–1007, https://doi.org/10.1021/es025910q, 2003.

Kenny, L. C., Gussman, R., and Meyer, M.: Development of a Sharp-Cut Cyclone for Ambient Aerosol Monitoring Applications, Aerosol Sci. Tech., 32, 338–358, https://doi.org/10.1080/027868200303669, 2000.

Khare, P., Machesky, J., Soto, R., He, M., Presto, A. A., and Gentner, D. R.: Asphalt-related emissions are a major missing nontraditional source of secondary organic aerosol precursors, Sci. Adv., 6, eabb9785, https://doi.org/10.1126/sciadv.abb9785, 2020.

Kleindienst, T. E., Jaoui, M., Lewandowski, M., Offenberg, J. H., and Docherty, K. S.: The formation of SOA and chemical tracer compounds from the photooxidation of naphthalene and its methyl analogs in the presence and absence of nitrogen oxides, Atmos. Chem. Phys., 12, 8711–8726, https://doi.org/10.5194/acp-12-8711-2012, 2012.

Knoderer, C., Nguyen, D., and Alrick, D.: 2017 Air Monitoring Network Plan, Bay Area Air Quality Management District, available at: https://www.baaqmd.gov/about-air-quality/air-quality-measurement/ambient-air-monitoring-network (last access: 29 September 2021), 2018.

Kreisberg, N. M., Worton, D. R., Zhao, Y., Isaacman, G., Goldstein, A. H., and Hering, S. V.: Development of an automated high-temperature valveless injection system for online gas chromatography, Atmos. Meas. Tech., 7, 4431–4444, https://doi.org/10.5194/amt-7-4431-2014, 2014.

Lamanna, M. S. and Goldstein, A. H.: In situ measurements of C2-C10 volatile organic compounds above a Sierra Nevada ponderosa pine plantation, J. Geophys. Res.-Atmos., 104, 21247–21262, https://doi.org/10.1029/1999JD900289, 1999.

Lerner, B. M., Gilman, J. B., Aikin, K. C., Atlas, E. L., Goldan, P. D., Graus, M., Hendershot, R., Isaacman-VanWertz, G. A., Koss, A., Kuster, W. C., Lueb, R. A., McLaughlin, R. J., Peischl, J., Sueper, D., Ryerson, T. B., Tokarek, T. W., Warneke, C., Yuan, B., and de Gouw, J. A.: An improved, automated whole air sampler and gas chromatography mass spectrometry analysis system for volatile organic compounds in the atmosphere, Atmos. Meas. Tech., 10, 291–313, https://doi.org/10.5194/amt-10-291-2017, 2017.

Lim, L. H., Harrison, R. M., and Harrad, S.: The Contribution of Traffic to Atmospheric Concentrations of Polycyclic Aromatic Hydrocarbons, Environ. Sci. Technol., 33, 3538–3542, https://doi.org/10.1021/es990392d, 1999.

Lim, Y. B. and Ziemann, P. J.: Effects of Molecular Structure on Aerosol Yields from OH Radical-Initiated Reactions of Linear, Branched, and Cyclic Alkanes in the Presence of NOx, Environ. Sci. Technol., 43, 2328–2334, https://doi.org/10.1021/es803389s, 2009.

Lopez-Hilfiker, F. D., Mohr, C., Ehn, M., Rubach, F., Kleist, E., Wildt, J., Mentel, Th. F., Lutz, A., Hallquist, M., Worsnop, D., and Thornton, J. A.: A novel method for online analysis of gas

and particle composition: description and evaluation of a Filter Inlet for Gases and AEROsols (FIGAERO), Atmos. Meas. Tech., 7, 983–1001, https://doi.org/10.5194/amt-7-983-2014, 2014.

Martinez, R. E., Williams, B. J., Zhang, Y., Hagan, D., Walker, M., Kreisberg, N. M., Hering, S. V., Hohaus, T., Jayne, J. T., and Worsnop, D. R.: Development of a volatility and polarity separator (VAPS) for volatility- and polarity-resolved organic aerosol measurement, Aerosol Sci. Tech., 50, 255–271, https://doi.org/10.1080/02786826.2016.1147645, 2016.

Millet, D. B., Donahue, N. M., Pandis, S. N., Polidori, A., Stanier, C. O., Turpin, B. J., and Goldstein, A. H.: Atmospheric volatile organic compound measurements during the Pittsburgh Air Quality Study: Results, interpretation, and quantification of primary and secondary contributions, J. Geophys. Res.-Atmos., 110, D07S07, https://doi.org/10.1029/2004JD004601, 2005.

Pollmann, J., Ortega, J., and Helmig, D.: Analysis of Atmospheric Sesquiterpenes: Sampling Losses and Mitigation of Ozone Interferences, Environ. Sci. Technol., 39, 9620–9629, https://doi.org/10.1021/es050440w, 2005.

Presto, A. A., Miracolo, M. A., Donahue, N. M., and Robinson, A. L.: Secondary Organic Aerosol Formation from High-NOx Photo-Oxidation of Low Volatility Precursors: n-Alkanes, Environ. Sci. Technol., 44, 2029–2034, https://doi.org/10.1021/es903712r, 2010.

Ren, H., Xue, M., An, Z., Zhou, W., and Jiang, J.: Quartz filter-based thermal desorption gas chromatography mass spectrometry for in-situ molecular level measurement of ambient organic aerosols, J. Chromatogr. A, 1589, 141–148, https://doi.org/10.1016/j.chroma.2019.01.010, 2019.

Robinson, A. L., Donahue, N. M., Shrivastava, M. K., Weitkamp, E. A., Sage, A. M., Grieshop, A. P., Lane, T. E., Pierce, J. R., and Pandis, S. N.: Rethinking Organic Aerosols: Semivolatile Emissions and Photochemical Aging, Science, 315, 1259–1262, https://doi.org/10.1126/science.1133061, 2007.

Seinfeld, J. H. and Pankow, J. F.: Organic Atmospheric Particulate Material, Annu. Rev. Phys. Chem., 54, 121–140, https://doi.org/10.1146/annurev.physchem.54.011002.103756, 2003.

Tenax® TA Breakthrough Volume Data, available at: https://www.sisweb.com/index/referenc/tenaxta.htm, last access: 20 March 2020.

Turpin, B. J., Saxena, P., and Andrews, E.: Measuring and simulating particulate organics in the atmosphere: problems and prospects, Atmos. Environ., 34, 2983–3013, https://doi.org/10.1016/S1352-2310(99)00501-4, 2000.

Wang, L., Atkinson, R., and Arey, J.: Dicarbonyl Products of the OH Radical-Initiated Reactions of Naphthalene and the C1- and C2-Alkylnaphthalenes, Environ. Sci. Technol., 41, 2803–2810, https://doi.org/10.1021/es0628102, 2007.

Weitkamp, E. A., Sage, A. M., Pierce, J. R., Donahue, N. M., and Robinson, A. L.: Organic Aerosol Formation from Photochemical Oxidation of Diesel Exhaust in a Smog Chamber, Environ. Sci. Technol., 41, 6969–6975, https://doi.org/10.1021/es070193r, 2007.

Williams, B. J., Goldstein, A. H., Kreisberg, N. M., and Hering, S. V.: An In-Situ Instrument for Speciated Organic Composition of Atmospheric Aerosols: Thermal Desorption Aerosol GC/MS-FID (TAG), Aerosol Sci. Tech., 40, 627–638, https://doi.org/10.1080/02786820600754631, 2006.

Williams, B. J., Goldstein, A. H., Kreisberg, N. M., Hering, S. V., Worsnop, D. R., Ulbrich, I. M., Docherty, K. S., and Jimenez, J. L.: Major components of atmospheric organic aerosol in southern California as determined by hourly measurements of source marker compounds, Atmos. Chem. Phys., 10, 11577–11603, https://doi.org/10.5194/acp-10-11577-2010, 2010.

Yee, L. D., Isaacman-VanWertz, G., Wernis, R. A., Meng, M., Rivera, V., Kreisberg, N. M., Hering, S. V., Bering, M. S., Glasius, M., Upshur, M. A., Gray Bé, A., Thomson, R. J., Geiger, F. M., Offenberg, J. H., Lewandowski, M., Kourtchev, I., Kalberer, M., de Sá, S., Martin, S. T., Alexander, M. L., Palm, B. B., Hu, W., Campuzano-Jost, P., Day, D. A., Jimenez, J. L., Liu, Y., McKinney, K. A., Artaxo, P., Viegas, J., Manzi, A., Oliveira, M. B., de Souza, R., Machado, L. A. T., Longo, K., and Goldstein, A. H.: Observations of sesquiterpenes and their oxidation products in central Amazonia during the wet and dry seasons, Atmos. Chem. Phys., 18, 10433–10457, https://doi.org/10.5194/acp-18-10433-2018, 2018.

Zhang, Q., Jimenez, J. L., Canagaratna, M. R., Allan, J. D., Coe, H., Ulbrich, I., Alfarra, M. R., Takami, A., Middlebrook, A. M., Sun, Y. L., Dzepina, K., Dunlea, E., Docherty, K., DeCarlo, P. F., Salcedo, D., Onasch, T., Jayne, J. T., Miyoshi, T., Shimono, A., Hatakeyama, S., Takegawa, N., Kondo, Y., Schneider, J., Drewnick, F., Borrmann, S., Weimer, S., Demerjian, K., Williams, P., Bower, K., Bahreini, R., Cottrell, L., Griffin, R. J., Rautiainen, J., Sun, J. Y., Zhang, Y. M., and Worsnop, D. R.: Ubiquity and dominance of oxygenated species in organic aerosols in anthropogenically-influenced Northern Hemisphere midlatitudes, Geophys. Res. Lett., 34, L13801, https://doi.org/10.1029/2007GL029979, 2007.

Zhao, Y., Kreisberg, N. M., Worton, D. R., Teng, A. P., Hering, S. V., and Goldstein, A. H.: Development of an In Situ Thermal Desorption Gas Chromatography Instrument for Quantifying Atmospheric Semi-Volatile Organic Compounds, Aerosol Sci. Tech., 47, 258–266, https://doi.org/10.1080/02786826.2012.747673, 2013.